

Effects of Doppler broadening on two-photon multiwave mixing

Barbara A. Capron and Murray Sargent III

Optical Sciences Center, University of Arizona, Tucson, Arizona 85721

(Received 31 March 1986)

We generalize the two-photon probe-absorption coefficient derived in a recent paper to include any amount of Doppler broadening and an arbitrarily intense saturator wave. The analysis is performed for both copropagating and counterpropagating pump and probe waves. By choosing a Lorentzian velocity distribution we are able to perform the integrals analytically and thus examine the transition from homogeneous broadening to extreme Doppler broadening both for zero and nonzero Stark shifts. We examine these transitions for both short coherence lifetimes and for coherence lifetimes approaching the population difference lifetime. For homogeneous broadening the probe-absorption spectrum has Rabi variations similar to the Mollow one-photon case. For Doppler widths much larger than the saturator Rabi flopping frequency, the probe-absorption spectrum for the bidirectional pump and probe approaches a Doppler-free Lorentzian with width equal to the homogeneous linewidth and center displaced by the dynamic Stark shift. For Doppler broadening as small as $1/2 T_2$, coherent dips fill in and Rabi variations disappear. We show for the bidirectional case that to second order for any degree of Doppler broadening or to any order for extreme Doppler broadening the absorption coefficient is Doppler-free. For the unidirectional case the Doppler-free conditions do not hold and the results are similar to those for one-photon inhomogeneous broadening and valid for two-photon running-wave inhomogeneous broadening.

I. INTRODUCTION

Two-photon Doppler-free spectroscopy is a commonly used technique in high-resolution spectroscopy. The first experiments using this method were performed by Bloembergen and Levenson¹ and Grynberg *et al.*² measuring hyperfine components in sodium, and many examples are given in the review articles by these two groups. Since then the technique has been used extensively, primarily with alkali-metal atoms, to measure fine-structure splittings, isotope shifts, Stark splittings, and high-lying Rydberg levels, and even to look at a number of molecules,³ including NH_3 and CH_3F . In techniques employing Doppler-free spectroscopy, moving atoms Doppler upshift one running wave while Doppler downshifting a counterpropagating wave an equal amount. Hence the Doppler shifts cancel for a two-photon transition induced by one photon from each of the two counterpropagating waves, and thereby result in a narrow absorption spectrum. Although this idea is widely accepted, it is in general only true to second order in the field amplitudes, and therefore may require low-intensity beams.

Three kinds of two-photon absorption configurations are shown in Fig. 1. In a recent letter⁴ we reported results for the second configuration for which the transmitted probe intensity is measured as a function of the probe tuning for counterpropagating pump and probe beams. We showed that for Doppler widths much larger than the saturator Rabi flopping frequency the probe-absorption spectrum approaches a Doppler-free Lorentzian with its center displaced by the dynamic Stark shift. In contrast for weaker Doppler broadening and no Stark shift, Rabi sidebands emerge ultimately producing an absorption spectrum⁵ reminiscent of the Mollow one-photon case.⁶

With a Stark shift the spectrum develops dispersive-like asymmetries. In this paper we generalize the two-photon probe-absorption coefficient for a homogeneously broadened medium subjected to an arbitrarily intense saturator wave to allow for Doppler broadening for both the case of the counterpropagating [Fig. 1(b)] and copropagating [Fig. 1(c)] pump and probe. An equivalent

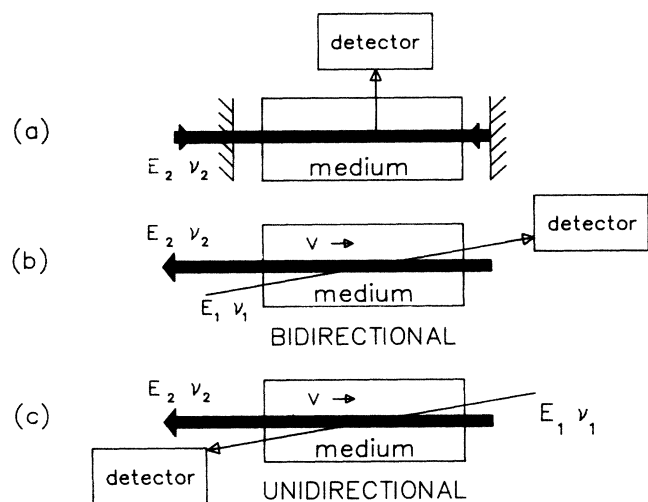


FIG. 1. Three configurations for two-photon absorption spectroscopy. In (a) intensity due to decay from upper level is measured as a function of laser tuning ν_2 . In (b) probe intensity is measured as a function of probe tuning ν_1 . Atoms with velocity v as shown will see ν_1 Doppler downshifted to $\nu_1 - Kv$ and ν_2 Doppler upshifted to $\nu_2 + Kv$. (c) Same as (b) except with copropagating beams both ν_1 and ν_2 are Doppler upshifted.

analysis for the one-photon case was presented in two papers by Baklanov and Chebotayev.^{7,8} For the unidirectional case the Doppler-free conditions do not hold and for zero Stark shifts and pump detuning the results correspond to those for the centrally tuned one-photon inhomogeneously broadened probe-absorption coefficient.⁹⁻¹¹ This unidirectional Doppler case is equivalent to a unidirectional inhomogeneously broadened case for stationary atoms. In Sec. II we review the two-photon two-level model used to obtain the probe-absorption coefficient. In order to include Doppler broadening we analytically integrate the absorption coefficient over a Lorentzian velocity distribution. The inclusion of Doppler broadening is discussed in Sec. III where the general answer for both the unidirectional and bidirectional cases is presented.

It is well known that the form of the absorption spectrum changes dramatically in different limits. For example the strong-field Mollow spectrum obtained when the level and coherence lifetimes are roughly equal transforms into the coherent dip spectrum with a weak field and a coherence lifetime much shorter than the population lifetime. In the rest of the paper we illustrate these limits numerically and show the effects of Doppler broadening. The formulas are evaluated and graphed on a personal computer. One of the interesting features occurring in multiphoton transitions is the dynamic Stark or level shift. As shown in Ref. 5 the existence of the Stark shift dramatically changes the absorption spectrum causing dispersivelike asymmetries similar to those caused by detuning. In Sec. IV we present results for the bidirectional case in these different limits for systems without Stark shifts and in Sec. V we show how Doppler broadening affects systems with Stark shifts and also those which are detuned. The same regimes for the unidirectional case are presented in Sec. VI. The Appendixes contain the full derivation of the bidirectional (Appendix A) and unidirectional (Appendix B) averages.

II. TWO-PHOTON TWO-LEVEL MODEL

The theory is based on the two-photon two-level scheme^{5,12,13} depicted in Fig. 2. We review the derivation of Ref. 5 here in order to familiarize the reader with both the theory and the notation. The electric dipole matrix element between the upper level a and the lower level b is zero, and the pump field at frequency ν_2 is approximately

TWO-PHOTON TWO-LEVEL DIAGRAM

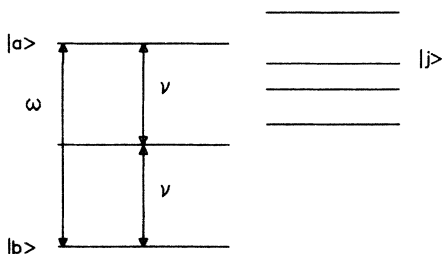


FIG. 2. Two-photon two-level model.

one half the frequency difference $\omega = \omega_a - \omega_b$. The intermediate levels j are assumed to be sufficiently non-resonant with the field frequencies that the $a \leftrightarrow j$ and $b \leftrightarrow j$ transitions can be accurately described by first-order perturbation theory and the j levels acquire no appreciable population. The probe field with amplitude \mathcal{E}_1 and frequency ν_1 must remain weak enough that saturation does not occur and both fields are treated classically.

In general the polarization of the medium with the level scheme in Fig. 2 is given by

$$P(\mathbf{r}, t) = N \text{tr}(\mathcal{O} \rho) = N \sum_j (\wp_{aj} \rho_{ja} + \wp_{bj} \rho_{jb}) + \text{c.c.}, \quad (1)$$

where \wp_{aj} is the electric dipole matrix element between the a and j states, \mathcal{O} is the atomic electric dipole operator, and ρ_{aj} is the density-matrix element between j and a . Since $a \leftrightarrow b$ is a two-photon transition, \wp_{ab} vanishes. For cases in which the polarization (1) is induced by the electric field

$$E(\mathbf{r}, t) = \frac{1}{2} \mathcal{E}(\mathbf{r}, t) e^{-i\nu t} + \text{c.c.}, \quad (2)$$

where $\mathcal{E}(\mathbf{r}, t)$ varies little in a time $1/\nu$, but may have rapid spatial variations like $\exp(i\mathbf{K} \cdot \mathbf{r})$ we obtain the polarization

$$P(\mathbf{r}, t) = \frac{1}{2} \mathcal{P}(\mathbf{r}, t) e^{-i\nu t} + \text{c.c.}, \quad (3)$$

where the complex polarization $\mathcal{P}(\mathbf{r}, t)$ also varies little in the time $1/\nu$. Combining Eqs. (1) and (3), we find

$$\mathcal{P}(\mathbf{r}, t) = 2N \sum_j (\wp_{aj} \rho_{aj} + \wp_{bj} \rho_{jb} + \text{c.c.}) e^{i\nu t}, \quad (4)$$

where we keep only terms varying little in an optical frequency period ($1/\nu$).

The electric dipole coherences ρ_{ja} are induced by the interaction energies

$$\mathcal{V}_{ja} = -\frac{1}{2\hbar} \wp_{ja} [\mathcal{E}(\mathbf{r}, t) e^{-i\nu t} + \text{c.c.}] \quad (5)$$

with a similar formula for ρ_{jb} . The equations of motion for ρ_{ja} and ρ_{jb} are obtained from the general Schrödinger equation of motion

$$\dot{\rho}_{ij} = -(\gamma_{ij} + i\omega_{ij})\rho_{ij} - i[\mathcal{V}, \rho]_{ij}, \quad (6)$$

where $\hbar\omega_{ij} = \hbar(\omega_i - \omega_j)$ is the energy difference between levels i and j and γ_{ij} is the corresponding decay constant. These equations are then integrated to first order in \mathcal{V} without making a rotating-wave approximation (RWA), since ν differs substantially from all $\pm\omega_{ja}$ and $\pm\omega_{jb}$, but $\omega_{ab} \equiv \omega_a - \omega_b \simeq 2\nu$ allowing us to replace terms like $\omega_{ja} + 3\nu$ with $\omega_{jb} + \nu$. Substituting the resulting expressions for ρ_{ja} and ρ_{jb} into the polarization (4) and keeping only terms that vary little in the time $1/\nu$ we have

$$\mathcal{P} = N \mathcal{E} (k_{aa} \rho_{aa} + k_{bb} \rho_{bb}) + 2N \mathcal{E}^* k_{ab}^* \rho_{ab} e^{2i\nu t}, \quad (7)$$

where the two-photon coefficients k_{ab} , k_{aa} , and k_{bb} are given by

$$k_{ab} = \hbar^{-1} \sum_j \wp_{aj} \wp_{jb} / (\omega_{jb} - \nu) \\ \simeq \hbar^{-1} \sum_j \wp_{aj} \wp_{jb} / (\omega_{ja} + \nu), \quad (8)$$

$$k_{aa} = 2\hbar^{-1} \sum_j |\wp_{ja}|^2 \omega_{ja} / (\omega_{ja}^2 - \nu^2), \quad (9)$$

$$k_{bb} = 2\hbar^{-1} \sum_j |\wp_{jb}|^2 \omega_{jb} / (\omega_{jb}^2 - \nu^2). \quad (10)$$

We then derive the "two-level" equations of motion for ρ_{aa} , ρ_{bb} , and ρ_{ab} using the expressions for ρ_{ja} and ρ_{jb} and the two-photon rotating-wave approximation, i.e., neglecting terms like $1/[\gamma + i(\omega + 2\nu)]$ compared to $1/[\gamma + i(\omega - 2\nu)]$. According to Eq. (6), we have

$$\dot{\rho}_{ab} = -(\gamma + i\omega)\rho_{ab} - i \sum_j (\mathcal{V}_{aj}\rho_{jb} - \rho_{aj}\mathcal{V}_{jb}), \quad (11)$$

$$\dot{\rho}_{aa} = -\gamma_a \rho_{aa} - \sum_j (i\mathcal{V}_{aj}\rho_{ja} + \text{c.c.}). \quad (12)$$

For simplicity we take $\dot{\rho}_{bb} = -\dot{\rho}_{aa}$, since we assume $\rho_{jj} = 0$. We likewise find the equation of motion for the population difference $D = \rho_{aa} - \rho_{bb}$,

$$\dot{D} = -(D + 1)/T_1 - 2 \sum_j (i\mathcal{V}_{aj}\rho_{ja} + \text{c.c.}), \quad (13)$$

where we write the population difference decay time $1/\gamma_a$ by its traditional NMR name T_1 . Substituting the values of ρ_{aj} and ρ_{bj} into (11), we have

$$\dot{\rho}_{ab} = -(\gamma + i\omega + i\omega_s I)\rho_{ab} - i(k_{ab}\mathcal{E}^2/4\hbar)e^{-2i\nu t}D, \quad (14)$$

where the two-photon dimensionless intensity

$$I = |k_{ab}\mathcal{E}^2| (T_1 T_2)^{1/2} / 2\hbar, \quad (15)$$

the two-photon coherence decay time $T_2 \equiv 1/\gamma$, and the Stark-shift parameter

$$\omega_s = (k_{bb} - k_{aa})/2 |k_{ab}| (T_1 T_2)^{1/2}. \quad (16)$$

Similarly we find

$$\dot{D} = -(D + 1)/T_1 + \frac{1}{2\hbar} (i\mathcal{E}^2 k_{ab} e^{-2i\nu t} \rho_{ba} + \text{c.c.}). \quad (17)$$

As discussed in Ref. 5, Eqs. (14) and (17) are the same as those for a one-photon two-level system with the substitutions

$$\omega \rightarrow \omega + \omega_s I, \quad \wp \mathcal{E} / \hbar \rightarrow k_{ab} \mathcal{E}^2 / 2\hbar, \quad \nu \rightarrow 2\nu. \quad (18)$$

These equations can be solved in steady state for single-frequency operation, but we are concerned here

with two waves. Thus, we suppose the electric field consists of two modes in the form

$$E(\mathbf{r}, t) = \frac{1}{2} [\mathcal{E}_1(\mathbf{r}) e^{i\Delta t} + \mathcal{E}_2(\mathbf{r})] e^{-i\nu_2 t} + \text{c.c.}, \quad (19)$$

i.e., the slowlyly varying complex field amplitude $\mathcal{E}(\mathbf{r}, t)$ is given by

$$\mathcal{E}(\mathbf{r}, t) = \mathcal{E}_1(\mathbf{r}) e^{i\Delta t} + \mathcal{E}_2(\mathbf{r}). \quad (20)$$

\mathcal{E}_2 is the pump-wave amplitude, while \mathcal{E}_1 is the probe-wave amplitude, and Δ is the pump-probe beat frequency $\nu_2 - \nu_1$. Similarly, we write the corresponding induced polarization in Eq. (3) as

$$\mathcal{P}(\mathbf{r}, t) = \mathcal{P}_1(\mathbf{r}) e^{i\Delta t} + \mathcal{P}_2(\mathbf{r}) + \mathcal{P}_3(\mathbf{r}) e^{-i\Delta t}. \quad (21)$$

Here we assume \mathcal{E}_1 is sufficiently small that other Fourier components of the polarization are negligible. As discussed in the single-photon theory, this occurs if $\mathcal{P}(\mathbf{r})$ is a linear function of \mathcal{E}_1 . To determine \mathcal{P} we need to solve the polarization (7) and equations of motion (14) and (17) to first-order in \mathcal{E}_1 , while keeping all orders in the pump amplitude \mathcal{E}_2 . As in the one-photon, two-level problem (see Ref. 9), it is clear that the field (19) induces a set of Fourier components in the two-photon coherence ρ_{ab} and in the probability difference D . Hence, we expand them in terms of these components. The assumption that \mathcal{E}_1 is weak limits these expansions to six Fourier coefficients. Thus we have

$$\rho_{ab} = e^{-2i(\nu_2 t - K_2 z)} \sum_m p_m e^{im[\Delta t - (K_2 - K_1)z]} \quad (22)$$

and

$$D = \sum_k d_k e^{ik[\Delta t - (K_2 - K_1)z]}, \quad (23)$$

which give

$$\rho_{ab} = \sum_m i p_m (m\Delta - 2\nu_2) e^{i[(m\Delta - 2\nu_2)t - m(K_2 - K_1)z - 2K_2 z]} \quad (24)$$

and

$$\dot{D} = \sum_k ik \Delta d_k e^{ik[\Delta t - (K_2 - K_1)z]}. \quad (25)$$

Substituting the truncated expansions (22) and (23) along with the field (19) into the polarization (7) and equating coefficients of $e^{i\Delta t}$ allows us to determine the slowly varying polarization $\mathcal{P}_1(\mathbf{r})$ and from it the complex absorption coefficient α_1 which is found to be

$$\alpha_1 = -i \frac{K_1 N}{4\epsilon_0} (k_{aa} + k_{bb}) + \frac{\alpha_0}{1 + I_2^2 \mathcal{L}_2} \left[-i\omega_s T_1 + I_2 \gamma \mathcal{D}_1 (2 - i\omega_s I_2 \mathcal{D}_2) \right. \\ \left. - I_2^2 (I_2 \gamma \mathcal{D}_1 - i\omega_s T_1) \mathcal{F}(\Delta) \gamma \frac{\mathcal{D}_1 + \mathcal{D}_2^* + \frac{1}{2} i\omega_s I_2 (\mathcal{D}_2^* \mathcal{D}_3^* - \mathcal{D}_1 \mathcal{D}_2)}{1 + I_2^2 \mathcal{F}(\Delta) \frac{\gamma}{2} (\mathcal{D}_1 + \mathcal{D}_3^*)} \right], \quad (26)$$

where α_0 is $K_2 N |k_{ab}| (T_2/T_1)^{1/2} / 2\epsilon_0$ and K_1 and K_2 are the wave numbers for modes 1 and 2. Other factors appearing in Eq. (26) are the two-photon complex denominator

$$\mathcal{D}_{2-m} = 1 / [\gamma + i(\omega + \omega_s I_2 - 2\nu_2 + m\Delta)], \quad (27)$$

the $m=0$ case of the Lorentzian

$$\mathcal{L}_{2-m} = 1 / [1 + (\omega + \omega_s I_2 - 2\nu_2 + m\Delta)^2 / \gamma^2], \quad (28)$$

and the population pulsation factor $\mathcal{F}(\Delta)$, which for this case equals $1/(1 + i\Delta T_1)$. The arrival at Eq. (26) brings us to the end of the review of the two-photon two-level theory. α_1 represents the complex absorption experienced by the probe at frequency ν_1 for the homogeneously broadened case. We now generalize it to include inhomogeneous, in particular, Doppler, broadening.

III. INCLUSION OF DOPPLER BROADENING

In order to generalize Eq. (26) to a Doppler-broadened medium we need to express α_1 as a function of velocity v and then integrate over the Doppler velocity distribution $W(v)$,

$$\langle \alpha_1 \rangle_{\text{DB}} = \int \alpha_1(v) W(v) dv. \quad (29)$$

We would normally expect $W(v)$ to be a Maxwellian distribution, but in order to perform the integral analytically we let $W(v)$ be the Lorentzian

$$W(v) = \frac{1}{\pi u} \frac{u^2}{u^2 + v^2}, \quad (30)$$

where $2u$ is the width of the velocity distribution. This distribution yields exact results in both the Doppler and homogeneously broadened limits and is a good approximation in between.

For moving atoms the time derivatives in the density matrix equations of motion become convective derivatives.¹⁴ Thus we have

$$\frac{d}{dt} \rightarrow \frac{\partial}{\partial t} + v_z \frac{\partial}{\partial z}, \quad (31)$$

where v_z is the component of velocity along the z axis. Using the expression in (31) for the derivative of (22) we obtain

$$\begin{aligned} \langle \alpha_1 \rangle_{\text{bd}} = & -\frac{iK_1 N}{4\epsilon_0} (k_{aa} + k_{bb}) + \alpha_0 (2I_2 \gamma \mathcal{D}_1 - i\omega_s T_1) \langle a_{11} \rangle - i\alpha_0 \omega_s I_2^2 \mathcal{D}_1 \langle a_{22} \rangle \\ & + \alpha_0 I_2^2 (i\omega_s T_1 - I_2 \gamma \mathcal{D}_1) \left[\gamma \mathcal{D}_1 \langle a_0 \rangle + \langle a_1 \rangle + \frac{i\omega_s I_2}{2\gamma} (\langle a_2 \rangle - \gamma \mathcal{D}_1 \langle a_3 \rangle) \right], \end{aligned} \quad (38)$$

where

$$\langle a_{11} \rangle = \frac{M(iw, \gamma)}{M(iw, \gamma')} + \frac{w}{\gamma'} \frac{\gamma^2 - \gamma'^2}{M(-i\gamma', w)}, \quad (39)$$

$$\langle a_{22} \rangle = -i\gamma \left[\frac{\Delta_2 + i(\gamma + w)}{M(iw, \gamma')} + \frac{iw}{\gamma'} \frac{\gamma + \gamma'}{M(-i\gamma', w)} \right], \quad (40)$$

$$\begin{aligned} \dot{\rho}_{ab} = & \sum_m i p_m [m\Delta - 2\nu_2 - v_z m (K_2 - K_1) + 2v_z K_2] \\ & \times e^{i[(m\Delta - 2\nu_2)t - m(K_2 - K_1)z + 2K_2 z]} \end{aligned} \quad (32)$$

For the case of copropagating probe and pump beams we let $K_2 \simeq K_1 \simeq -K$ where

$$K |v_z| = (\nu_2/c) |v_z| \simeq (\nu_1/c) |v_z|, \quad (33)$$

and substituting this into Eq. (32) we obtain

$$\dot{\rho}_{ab} = \sum_m i p_m (m\Delta - 2\nu_2 - 2Kv_z) e^{i[(m\Delta - 2\nu_2)t - 2Kz]}. \quad (34)$$

By letting

$$\nu'_2 = \nu_2 + Kv_z$$

and

$$(35)$$

$$\nu'_1 = \nu_1 + Kv_z$$

in the coefficients in Eq. (34) we retrieve Eq. (24). We find the same result for the \dot{D} equation (Eq. 25). Thus we can obtain $\alpha_1(v)$ for the unidirectional case by performing the substitutions of Eqs. (35) in Eq. (26).

Likewise we do a similar substitution for the bidirectional case where we let $K_1 \simeq -K_2 \simeq K$ in Eq. (32). We then obtain

$$\begin{aligned} \dot{\rho}_{ab} = & \sum_m i p_m [m\Delta - 2\nu_2 + 2(m-1)Kv_z] \\ & \times e^{i[(m\Delta - 2\nu_2)t + 2(m-1)Kz]}. \end{aligned} \quad (36)$$

In this case if we let

$$\nu'_2 = \nu_2 + Kv_z$$

and

$$(37)$$

$$\nu'_1 = \nu_1 - Kv_z$$

in the coefficients we again retrieve Eq. (24). The same can be done for Eq. (23) to obtain \dot{D} and thus for the bidirectional case we obtain $\alpha_1(v)$ by substituting Eqs. (37) into Eq. (24). To find the average over the velocity distribution $W(v)$, we use the appropriate $\alpha_1(v)$ in Eq. (29).

The Appendixes carry out the averages for a Lorentzian velocity distribution for both unidirectional and bidirectional cases using the calculus of residues and we just give the results here. For the bidirectional case we have

$$\langle a_0 \rangle = -B \left[\frac{M(iw, \gamma)G(-iw)}{M(iw, \gamma')} + \frac{w}{\gamma'} \frac{(\gamma^2 - \gamma'^2)G(\Delta_2 - i\gamma')}{M(-i\gamma', w)} \right], \quad (41)$$

$$\langle a_1 \rangle = -i\gamma B \left[\frac{\Delta_2 + i(w - \gamma)}{M(iw, \gamma')} G(-iw) + \frac{iw}{\gamma'} \frac{(\gamma' - \gamma)G(\Delta_2 - i\gamma')}{M(-i\gamma', w)} \right], \quad (42)$$

$$\langle a_2 \rangle = \gamma^2 B \left[\frac{[\Delta_2 + i(w - \gamma)]G(-iw)}{[\Delta_2 - \Delta + i(2w + \gamma)]M(iw, \gamma')} - \frac{iw}{\gamma'} \frac{(\gamma' - \gamma)G(\Delta_2 - i\gamma')}{[\Delta_2 + \Delta - i(2\gamma' + \gamma)]M(-i\gamma', w)} \right], \quad (43)$$

and

$$\langle a_3 \rangle = i\gamma B \left[\frac{\Delta_2 + i(w + \gamma)}{M(iw, \gamma')} G(-iw) + \frac{iw}{\gamma} (\gamma' + \gamma) \frac{G(\Delta_2 - i\gamma')}{M(-i\gamma', w)} \right], \quad (44)$$

where $M(iw, \gamma)$ is given by Eq. (A15) as $M(iw, \gamma) = (\Delta_2 + iw)^2 + \gamma^2$ and $G(iw)$ is given by Eq. (A30). In practice for the Doppler-broadened limit where $w \rightarrow \infty$, we have $M(\pm iw, \gamma) \rightarrow -w^2$, $M(\pm i\gamma, w) \rightarrow w^2$, and $G(-iw) \rightarrow 0$ causing all the $\langle a_n \rangle$ except $\langle a_{11} \rangle$ to be zero thus giving us the Doppler-free expression given in Ref. 4.

For the unidirectional case we obtain

$$\begin{aligned} \langle \alpha_1 \rangle_{\text{ud}} = & -\frac{iK_1 N}{4\epsilon_0} (k_{aa} + k_{bb}) + \alpha_0 (-i\omega_s T_1 \langle b_{11} \rangle + 2I_2 \langle b_{22} \rangle - iI_2^2 \langle b_{33} \rangle) \\ & - I_2^2 \mathcal{F}(\Delta) \alpha_0 \left[I_2 \langle b_1 \rangle - i\omega_s T_1 \langle b_2 \rangle + \frac{iI_2^2}{2} (\langle b_3 \rangle - \langle b_4 \rangle) + \frac{\omega_s T_1 I_2}{2} (\langle b_5 \rangle - \langle b_6 \rangle) \right], \end{aligned} \quad (45)$$

where

$$\langle b_{11} \rangle = \frac{M(-iw, \gamma)}{M(-iw, \gamma')} + \frac{w}{\gamma'} \frac{\gamma^2 - \gamma'^2}{M(i\gamma', w)}, \quad (46)$$

$$\langle b_{22} \rangle = \frac{i\gamma}{[-\Delta_2 - \Delta + i(w + \gamma)]} \frac{M(-iw, \gamma)}{M(-iw, \gamma')} + \frac{w}{\gamma'} \frac{i\gamma(\gamma^2 - \gamma'^2)}{[-\Delta + i(\gamma' + \gamma)]M(i\gamma', w)}, \quad (47)$$

$$\langle b_{33} \rangle = \frac{-\omega_s \gamma [-\Delta_2 + i(w - \gamma)]}{[-\Delta_2 - \Delta + i(w + \gamma)]M(-iw, \gamma')} - \frac{iw}{\gamma'} \frac{\omega_s \gamma (\gamma' - \gamma)}{[-\Delta_2 - \Delta + i(\gamma' + \gamma)]M(i\gamma', w)}, \quad (48)$$

$$\begin{aligned} \langle b_1 \rangle = & \frac{i\gamma^2(2\gamma + i\Delta)[- \Delta_2 + \Delta + i(w - \gamma)][- \Delta_2 + i(w + \gamma)]}{[- \Delta_2 - \Delta + i(w + \gamma)]M(-iw, \gamma')N(iw)} - \frac{w}{\gamma'} \frac{\gamma^2(2\gamma + i\Delta)(\gamma' + \gamma)[\Delta + i(\gamma' - \gamma)]}{[- \Delta + i(\gamma' + \gamma)]M(i\gamma', w)N(\Delta_2 + i\gamma')} \\ & - 2w \frac{\gamma^2(2\gamma + i\Delta)(- \Delta_2 + \Delta - i\gamma + \beta_1)(- \Delta_2 + i\gamma + \beta_1)}{(- \Delta_2 - \Delta + i\gamma + \beta_1)M(-\beta_1, \gamma')Q}, \end{aligned} \quad (49)$$

$$\begin{aligned} \langle b_2 \rangle = & \frac{\gamma(2\gamma + i\Delta)[- \Delta_2 + \Delta + i(w - \gamma)][- \Delta_2 + i(w + \gamma)]}{M(-iw, \gamma')N(iw)} + \frac{iw}{\gamma'} \frac{\gamma(2\gamma + i\Delta)(\gamma' + \gamma)[\Delta + i(\gamma' - \gamma)]}{M(i\gamma', w)N(\Delta_2 + i\gamma')} \\ & + 2iw \frac{\gamma(2\gamma + i\Delta)(- \Delta_2 + \Delta - i\gamma + \beta_1)(- \Delta_2 + i\gamma + \beta_1)}{M(-\beta_1, \gamma')Q}, \end{aligned} \quad (50)$$

$$\langle b_3 \rangle = -i \frac{\gamma^2 \omega_s [-\Delta_2 + i(w + \gamma)]}{M(-iw, \gamma')N(iw)} + \frac{w}{\gamma'} \frac{\gamma^2 \omega_s (\gamma' + \gamma)}{M(i\gamma', w)N(\Delta_2 + i\gamma')} + 2w \frac{\gamma^2 \omega_s (-\Delta_2 + i\gamma + \beta_1)}{M(-\beta_1, \gamma')Q}, \quad (51)$$

$$\begin{aligned} \langle b_4 \rangle = & \frac{-i\gamma^2 \omega_s [-\Delta_2 + \Delta + i(w - \gamma)][- \Delta_2 + i(w - \gamma)]}{[- \Delta_2 - \Delta + i(w + \gamma)]M(-iw, \gamma')N(iw)} + \frac{w}{\gamma'} \frac{\gamma^2 \omega_s (\gamma' - \gamma)[\Delta + i(\gamma' - \gamma)]}{[- \Delta + i(\gamma' + \gamma)]M(i\gamma', w)N(\Delta_2 + i\gamma')} \\ & + 2w \frac{\gamma^2 \omega_s (-\Delta_2 + \Delta - i\gamma + \beta_1)(- \Delta_2 - i\gamma + \beta_1)}{(- \Delta_2 - \Delta + i\gamma + \beta_1)M(-\beta_1, \gamma')Q}, \end{aligned} \quad (52)$$

$$\begin{aligned} \langle b_5 \rangle = & -\frac{\gamma \omega_s [-\Delta_2 - \Delta + i(w + \gamma)][- \Delta_2 + i(w + \gamma)]}{M(-iw, \gamma')N(iw)} - \frac{iw}{\gamma'} \frac{\gamma \omega_s (\gamma' + \gamma)[-\Delta + i(\gamma' + \gamma)]}{M(i\gamma', w)N(\Delta_2 + i\gamma')} \\ & - 2iw \frac{\gamma \omega_s (-\Delta_2 - \Delta + i\gamma + \beta_1)(- \Delta_2 + i\gamma + \beta_1)}{M(-\beta_1, \gamma')Q}, \end{aligned} \quad (53)$$

and

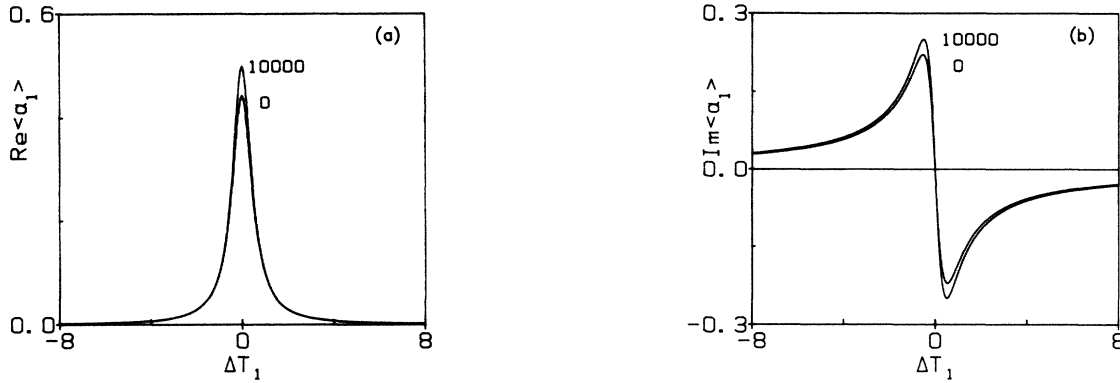


FIG. 3. (a) Real part of $\langle \alpha_1 \rangle_{bd}$ vs ΔT_1 for $I_2=0.25$ for homogeneous ($wT_1=0$) and extreme Doppler ($wT_1=10000$) broadening. $T_2=2T_1$. (b) The imaginary part for the same parameters.

$$\langle b_6 \rangle = -\frac{\gamma \omega_s [-\Delta_2 + \Delta + i(w - \gamma)] [-\Delta_2 + i(w - \gamma)]}{M(-iw, \gamma') N(iw)} - \frac{iw \gamma \omega_s (\gamma' - \gamma) [\Delta + i(\gamma' - \gamma)]}{\gamma' M(i\gamma', w) N(\Delta_2 + i\gamma')} - 2iw \frac{\gamma \omega_s (-\Delta_2 + \Delta - i\gamma + \beta_1) (-\Delta_2 - i\gamma + \beta_1)}{M(-\beta_1, \gamma') Q}. \quad (54)$$

The expressions for M , B , G , β_1 , N , and Q which appear in Eqs. (39)–(54) are given in the Appendixes in Eqs. (A15), (A28), (A30), (B20), (B35), and (B36), respectively.

The general expression for $\langle \alpha_1 \rangle_{ud}$ simplifies substantially in the extreme Doppler limit. Since the unidirectional case is not Doppler free one needs to normalize by multiplying by $Z = (w + \gamma)/\gamma$ to prevent all terms from vanishing in this limit. After the Z normalization, the first and third terms in Eqs. (51)–(56) and the first term in Eq. (50) all go to zero. The general expressions for $\langle \alpha_1 \rangle$ [Eqs. (38) and (45)] can be evaluated for any degree of Doppler broadening by merely changing the value of w , the width of the Doppler distribution.

IV. BIDIRECTIONAL RESULTS: ZERO STARK SHIFTS

In Secs. IV and V we examine the results for the bidirectional pump and probe. To second order in the

strong field, the probe absorption coefficient (26) approaches the simple form^{4,15}

$$\alpha_1 \approx \alpha_0 (2\gamma \mathcal{D}_1 I_2 - i\omega_s T_1), \quad (55)$$

aside from the constant index term proportional to $k_{aa} + k_{bb}$. This is the identical result found for the probe-absorption coefficient in the extreme Doppler limit, which confirms the well-known result that for low intensities the absorption spectrum is Doppler-free. Thus, in this low-intensity limit we do not expect the degree of Doppler broadening to affect the width of the Lorentzian. This is borne out in Fig. 3(a) which shows the real part of the probe-absorption spectrum as a function of pump-probe detuning for the dimensionless intensity $I_2=0.25$ and for two different velocity distribution widths w , expressed in units of $1/T_1$. The case for $w=0$ is the homogeneous limit and $w=10000$ gives the Doppler limit within the resolution of the graphs. The curves are nearly identical,

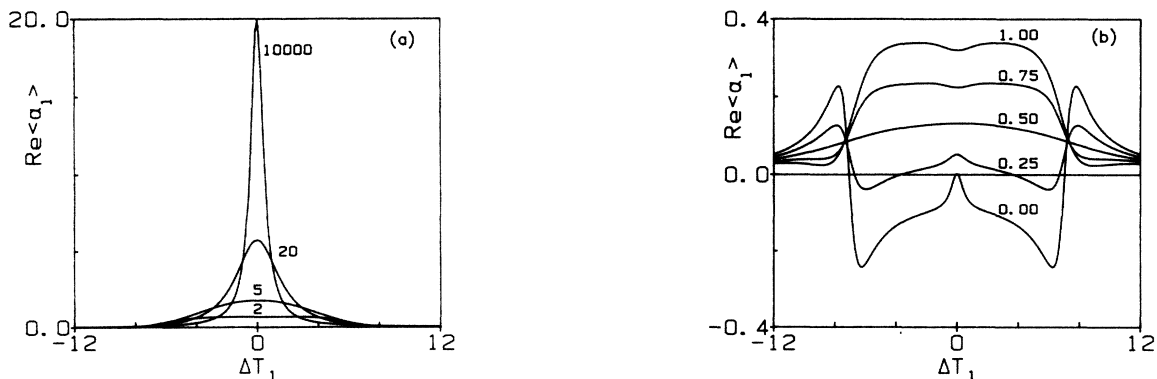


FIG. 4. $\text{Re}\langle \alpha_1 \rangle_{bd}$ vs ΔT_1 for $I_2=10$ for decreasing amounts of Doppler broadening from the Doppler limit to the homogeneous limit. (a) $wT_1=2, 5, 20,$ and 10000 . (b) $wT_1=0, 0.25, 0.5, 0.75,$ and 1.0 . In both cases $T_2=2T_1$.

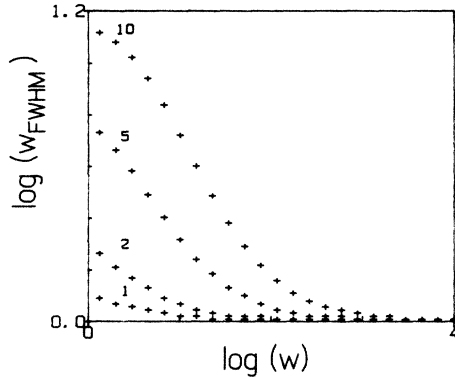


FIG. 5. $\log(w_{\text{FWHM}})$ vs $\log(w)$ for $I_2=1, 2, 5,$ and 10 .

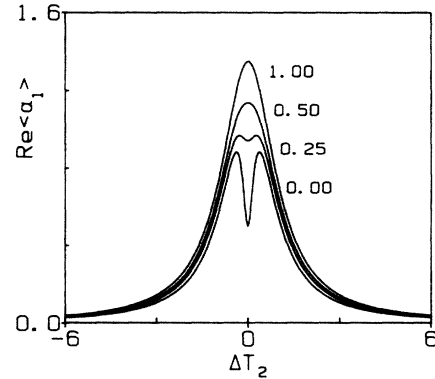


FIG. 6. $\text{Re}\langle\alpha_1\rangle_{\text{bd}}$ vs ΔT_2 in the coherent-dip limit for $wT_2=0, 0.25, 0.5,$ and 1 . $I_2=1$ and $T_1=10T_2$.

differing only in the height of the absorption peak. This difference is caused by the fact that in the Doppler limit relatively fewer atoms are saturated than in the homogeneous limit where all the atoms are saturated. Figure 3(b) shows the imaginary part of α_1 for the same parameters and again there is very little difference between the two limits.

This result is strikingly different from that for a high-intensity field in the homogeneous limit⁴ where the two-photon absorption spectrum has the same shape as the one-photon result of Mollow with wide wings out past the Rabi sidebands and negative regions corresponding to gain. As demonstrated in Figs. 4(a) and 4(b), as the Doppler width is increased to $0.5\gamma_a$ the Rabi wiggles vanish but the spectrum remains power broadened. When the Doppler limit is reached the spectrum has narrowed to the Doppler-free Lorentzian of width $2/T_2$ but substantial Doppler broadening is needed to overcome the power broadening and approach this width. In order to more thoroughly examine the width of the Lorentzian as a function of Doppler broadening we have calculated the full width at half maximum (w_{FWHM}) of the absorption spectrum for several values of the intensity. The results are presented in Fig. 5 which shows in log-log form w_{FWHM} plotted against the Doppler width w for four different intensities I_2 . Of course, this particular measure really has no meaning for the cases in which the spectrum

is not bell shaped so for each curve we have limited the minimum Doppler width w which is allowed. However that part of the curve is well away from the region where the Doppler limit is approach. We can see that as the intensity is increased so too is the Doppler width required to reach the Doppler-free Lorentzian.

The previous results have all been for the limit where the population difference and coherence lifetimes have the same order of magnitude. We now examine the limit where the coherence lifetime T_2 is much shorter than the population difference lifetime T_1 . This regime is known as the coherent-dip limit because the absorption spectrum shows a dip reminiscent of the Lamb dip but of a completely different origin. The coherent dip is caused by the fact that population pulsations have a limited bandwidth given approximately by $(1+I_2^2)/T_1$. The coherent dip as such only occurs for low intensities, evolving into the Mollow-type spectrum as the intensity increases. We examine this regime for both high and low intensities. Figure 6 shows the real part of α_1 as a function of pump-probe detuning (now in units of $1/T_2$) as the Doppler width is increased. It can be seen that the coherent dip is nearly immediately wiped out. By the time $w=1/2T_2$ there is no longer any evidence of a dip. This result is expected physically since the dip is due to the atomic response to the coherent superposition between the two

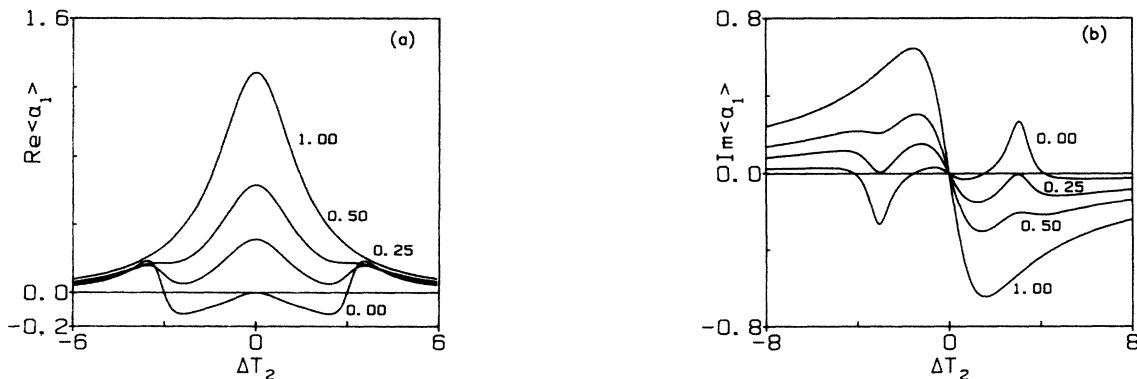


FIG. 7. $\langle\alpha_1\rangle_{\text{bd}}$ vs ΔT_2 in the high intensity ($I_2=10$), short dipole lifetime ($T_1=10T_2$) limit. (a) $\text{Re}\langle\alpha_1\rangle_{\text{bd}}$ for $wT_2=0, 0.25, 0.5,$ and 1 . (b) $\text{Im}\langle\alpha_1\rangle_{\text{bd}}$ for the same parameters.

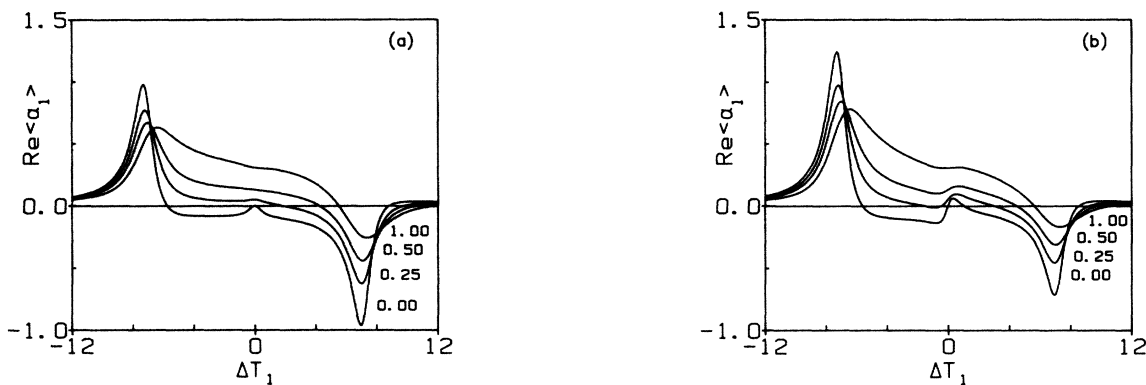


FIG. 8. $\text{Re}\langle\alpha_1\rangle_{\text{bd}}$ vs ΔT_1 in the high intensity ($I_2=10$) regime when the lifetimes are on the same order ($T_2=2T_1$) for $wT_1=0, 0.25, 0.5$, and 1 . (a) $\omega_S T_1=0.1$ and $\delta_2 T_1 \equiv (\omega - 2\nu_2)T_1=0$. (b) $\omega_S T_1=0$ and $\delta_2 T_1=1$.

fields (fringe pattern) and with any degree of Doppler broadening the atoms see only an average field.

As mentioned above the coherent dip is only a low-intensity phenomenon. In the high-intensity regime the curves resemble those for equal lifetimes as shown in Ref. 4. We illustrate this regime in Fig. 7(a) which shows the Rabi sidebands rapidly vanishing as coherent effects are wiped out and the Doppler-free Lorentzian is approached. The lack of power broadening in the extreme Doppler limit is due to the fact that in this case only a small fraction of the atoms experience saturation whereas with a small degree of Doppler broadening a larger fraction of the atoms are saturated. We also present the imaginary part of α_1 in this limit in Fig. 7(b). It shows how multiple regions of anomalous dispersion obtained in the homogeneous limit rapidly vanish as the standard dispersive-type curve is reached for w as small as γ .

V. BIDIRECTIONAL RESULTS: NONZERO STARK SHIFTS AND DETUNING

In this section we examine the effects of Stark shifts and detunings from the atomic resonance frequency in the various limits examined in Sec. IV, still for the bidirectional case. Stark shifts which are inherent to many two-photon systems, particularly in Rydberg atoms, add a degree of complexity unique to multiphoton problems. In

general both Stark shifts and detunings cause asymmetries to appear in the otherwise symmetric absorption spectra. Often the effects of the Stark shift and detuning are very similar since the Stark-shift term frequently occurs in the argument of a Lorentzian. Such is the case for the low-intensity limit discussed below. However, as shown in Eq. (26) the Stark shift also occurs outside of arguments and then causes effects markedly different from simple detunings.

We first examine the limit where T_1 and T_2 have the same order of magnitude. In the weak-field case the Stark shift is insignificant because as seen in Eq. (55) ω_S only occurs multiplied by I_2 in the argument of \mathcal{D}_1 and only causes a very slight shift of the Lorentzian, as long as $\omega_S I_2$ is not comparable or large relative to γ . Stark shifts do have a marked effect on the strong-field-absorption spectrum for the homogeneously broadened case, where once again the effect is very similar to that caused by detuning, and the changes caused by Doppler broadening in the two are also very similar. This is illustrated in Figs. 8(a) and 8(b) where we show the real part of α_1 with $\omega_S T_1=0.1$ and $(\omega - 2\nu_2)T_1=0$ in (a) and $(\omega - 2\nu_2)T_1=0.1$ while $\omega_S T_1=0$ in (b). Both are shown for several values of the Doppler width w and $I_2=10$. Both sets of curves are remarkably similar and vary in the same manner as w is increased. In particular, for the homogeneously broadened case a Stark shift or detuning causes

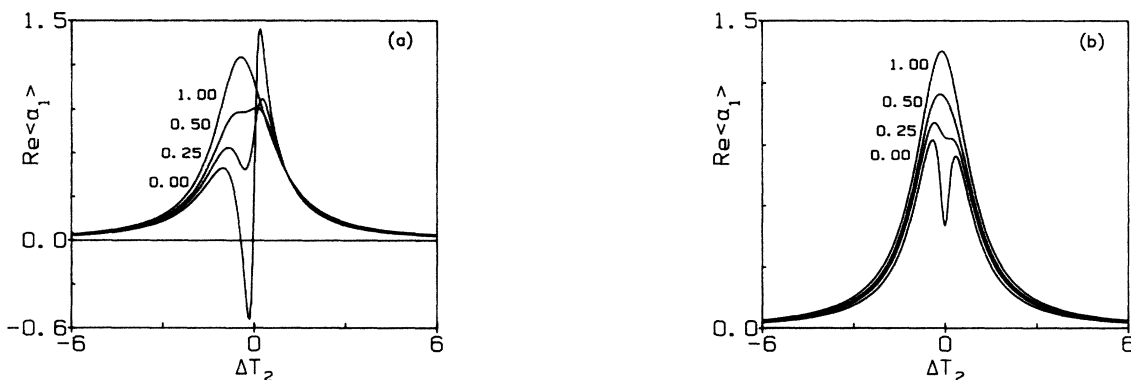


FIG. 9. Same as Fig. 6 except in (a) $\omega_S T_2=0.5$ and $\delta_2 T_2=0$. (b) $\omega_S T_2=0$ while $\delta_2 T_2=0.1$.

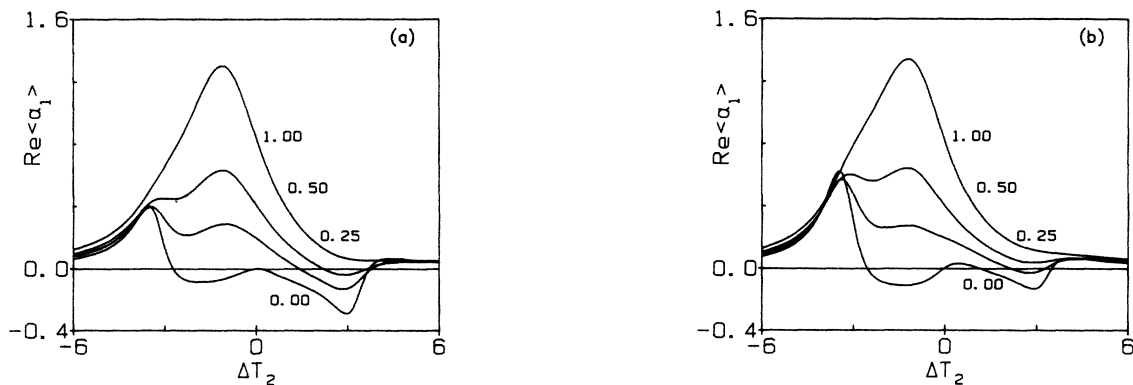


FIG. 10. Same as Fig. 7(a) except in (a) $\omega_S T_2 = 0.1$ and $\delta_2 T_2 = 0$. (b) $\omega_S T_2 = 0$ and $\delta_2 T_2 = 0.1$.

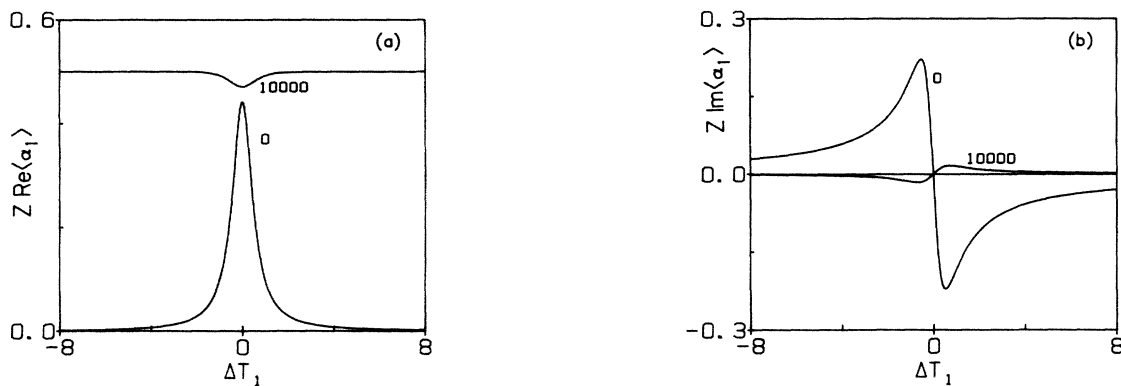


FIG. 11. The real (a) and imaginary (b) parts of $Z \langle \alpha_1 \rangle_{ud}$ for homogeneous ($\omega T_1 = 0$) and inhomogeneous ($\omega T_1 = 10000$) broadening. Other parameters the same as in Fig. 3.

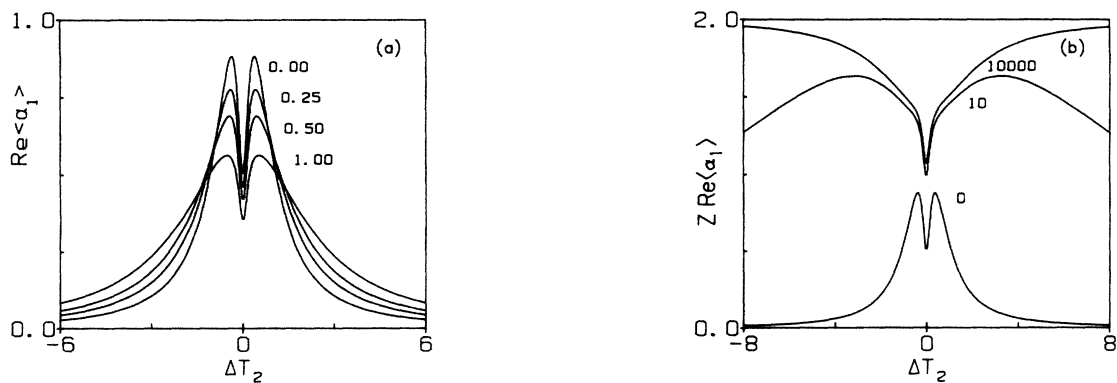


FIG. 12. (a) $\text{Re} \langle \alpha_1 \rangle_{ud}$ for the same parameters as in Fig. 6. (b) The same except scaled by Z and showing the homogeneously ($\omega T_2 = 0$), intermediately ($\omega T_2 = 10$) broadened and inhomogeneously ($\omega T_2 = 10000$) broadened limits.

the gain of one Rabi sideband to turn into an absorption peak while causing that of the other to grow. When Doppler broadening is taken into account, as the width of the Doppler distribution increases, the asymmetry disappears. The absorption peak initially broadens and shifts inward away from the Rabi frequency while the gain vanishes. As in the zero Stark-shift case, as the Doppler limit is approached, the spectrum reaches the $2/T_2$ width predicted in Eq. (55). In the extreme Doppler-limit Stark shifts or detuning merely displace the Doppler-free Lorentzian from its zero-Stark-shift location.

We now examine the regime where $T_2 \ll T_1$. As shown in Sec. IV, for the low-intensity limit, the coherent dip found in the homogeneously broadened case is filled in by Doppler broadening larger than $1/2T_2$. The same is true when Stark shifts or detuning are included as is illustrated in Figs. 9(a) and 9(b). In this case while the effect of the detuning and the Stark shift are quite dissimilar in the homogeneously broadened limit (a phenomenon which we will examine more closely in a forthcoming paper) as the broadening is increased the curves once again approach the same shape of the shifted Lorentzian. The final case to be examined is the strong-field limit for these lifetimes. The transition from homogeneously to Doppler broadened for both a Stark-shifted but centrally tuned and a detuned system with no Stark shift are shown in Figs. 10(a) and 10(b) where once again the effect of detuning and Stark shifting are very similar, and once again the asymmetries appearing in the homogeneously broadened case disappear as the Doppler broadening is increased.

VI. UNIDIRECTIONAL RESULTS

The probe-absorption coefficient averaged over Doppler broadening for a unidirectional pump and probe contrasts substantially with the counterpropagating case. It is equivalent to unidirectional non-Doppler inhomogeneous broadening. Also, due to the similarity between the one- and two-photon theories it is of interest to compare the results to those for one-photon inhomogeneous broadening. In this section we present the unidirectional results in the same limits that were examined above for the bidirectional case. In general the unidirectional absorption coefficient does not approach a Lorentzian. To prevent $\langle \alpha_1 \rangle$ from vanishing in the extreme Doppler limit and yet still reduce to the correct homogeneous value for $w=0$, we have normalized some of the following results by multiplying $\langle \alpha_1 \rangle$ by $Z = (w + \gamma)/\gamma$.¹⁰

First we examine the results for zero Stark shifts and zero detuning. As shown in Appendix B, in the unidirectional case \mathcal{D}_1 is no longer independent of velocity and is therefore not Doppler free. Thus Eq. (55) no longer describes the Doppler-broadened result. In Fig. 11 we present the results for the two limiting cases of homogeneous and extreme Doppler broadening for a low-intensity pump. All parameters are the same as those for Fig. 3 except here we have normalized by multiplying by Z . As required, the homogeneously broadened results are identical for the two cases, but for the copropagating pump and probe, in the extreme Doppler limit, we obtain for the real part of α_1 a slight dip instead of a Lorentzian peak and

for the imaginary part a slight dispersive-type curve of opposite sign.

We next examine the low-intensity limit with a short coherence lifetime. Figure 12(a), corresponding to the bidirectional case of Fig. 6 with the same parameters, shows the change caused by slight Doppler broadening. The coherent dip is not filled in as it was before, and in fact as shown in Fig. 12(b) (which is Z normalized) even when we reach the extreme Doppler limit, there is still a dip. Since the filling in of the dip depends on the angle between pump and probe, it offers a means of measuring the diffusion of atoms through the system by varying the pump-probe angle.

Now we examine the short-coherence-lifetime limit for

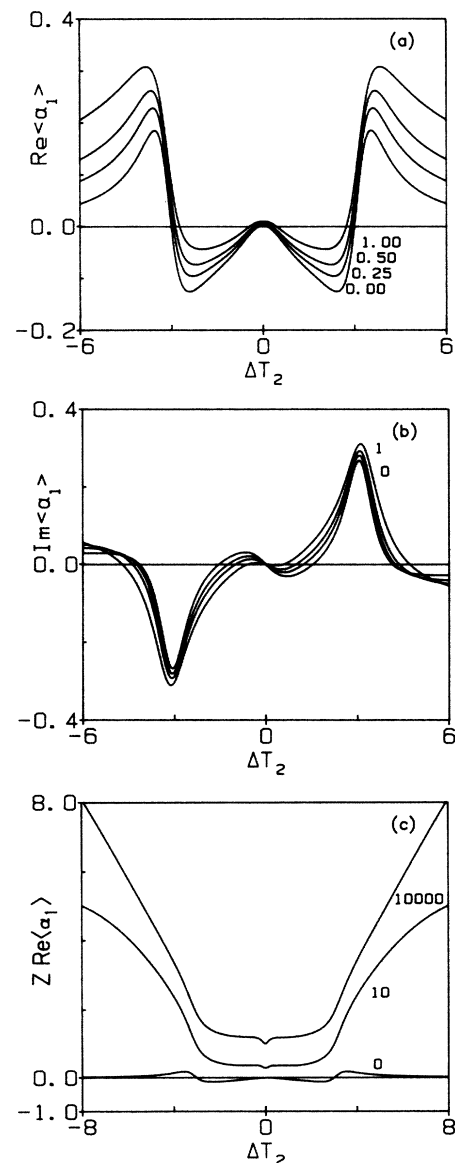


FIG. 13. $\langle \alpha_1 \rangle_{ud}$ vs ΔT_2 for the large intensity, short dipole lifetime limit. (a) The real and (b) the imaginary parts. All parameters are the same as in Fig. 7. (c) $Z \text{Re}(\alpha_1)$ for the homogeneous ($wT_2=0$) and inhomogeneous ($wT_2=10000$) limits. All other parameters as in (a).

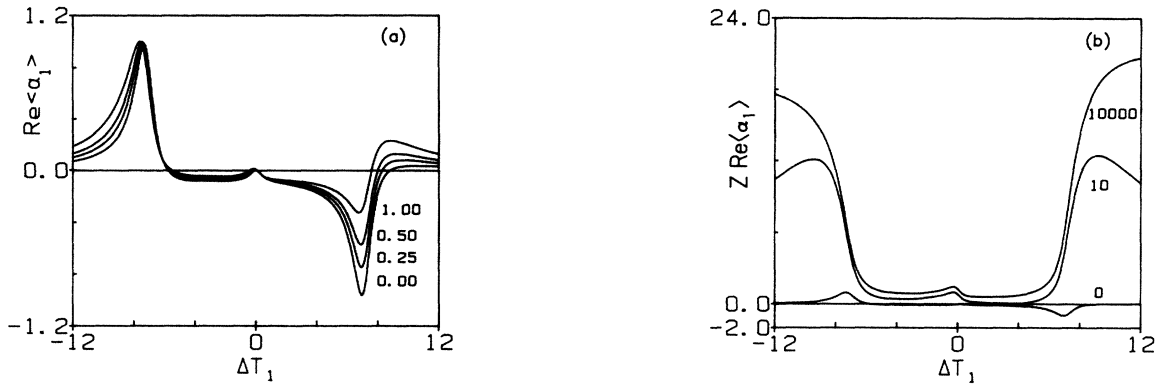


FIG. 14. (a) $\text{Re}\langle\alpha_1\rangle_{ud}$ vs ΔT_1 for $\omega_S T_1 = 0.1$. All other parameters the same as in Fig. 8(a). (b) The same as (a) except scaled by Z and for the homogeneously ($\omega T_1 = 0$), intermediately ($\omega T_1 = 10$), and inhomogeneously ($\omega T_1 = 10000$) broadened limits.

a high-intensity pump. Figures 13(a) and 13(b) correspond to Figs. 7(a) and 7(b) for the bidirectional case. In the previous case the Rabi variations rapidly vanished and the curve was bell shaped by the time ω reached γ . In this case the Rabi variations remain and turn into the broad shoulders shown in Fig. 13(c) (Z normalized) for the extreme Doppler limit. This figure is very reminiscent of those in Ref. 11 showing extreme inhomogeneous broadening for the one-photon case. This is not surprising since Eqs. (45), (47), and (49) in the limit where $\omega_s = \Delta_2 = 0$ correspond to the formulas presented in Ref. 10 [Eq. (22)] for the one-photon semiclassical inhomogeneously broadened probe-absorption coefficient except for some extra factors of I_2 in the two-photon case. The average over velocities for a copropagating pump and probe is thus equivalent to an average over different line centers except that for this case we still have remaining after the average the degrees of freedom represented by the detuning from the atomic line center and Stark shifts. We next examine the effects caused by changing these two parameters but first mention that the curves for nearly equal lifetimes and a strong pump are very similar to Fig. 13 with the exception that in the Doppler limit, the dip seen for the short coherence lifetime turns into a slight peak in the other regime.

Figure 14(a) shows the absorption coefficient for the

same parameters as in Fig. 8(a) (strong field, $T_2 = 2T_1$) for the bidirectional case with a Stark shift of $1/10T_1$. Here the dispersive-like asymmetries do not disappear but merely decrease somewhat in intensity. The effect of detuning with no Stark shift is similar to that of a Stark shift with no detuning, as in the bidirectional case. In Fig. 14(b) (Z normalized) we show the extreme Doppler limit with the small Stark shift. Again we see the broad shoulders except that one is slightly higher than the other. For a slight detuning with no Stark shift we obtain a similar curve except that the shoulders are once again equal.

Figure 9 shows the difference between a small atomic detuning and a slight Stark shift in the limits of short coherence lifetimes and a weak pump (coherent-dip limit) for Doppler broadening up to $1/T_2$. We show the equivalent (except Z normalized) curves for the unidirectional case in Figs. 15(a) and 15(b). Now neither the dip seen for small detuning nor the dispersive characteristic seen for small Stark shifts vanish but rather both stay at the same intensity. To show what happens in the Doppler limit we have Figs. 16(a) and 16(b) which are also Z normalized. There we see that both the dip and the sharp dispersive shape remain.

Finally we examine the difference between detuning and Stark shifting for long population lifetimes and strong pumps. As in the bidirectional case shown in Figs. 10(a)

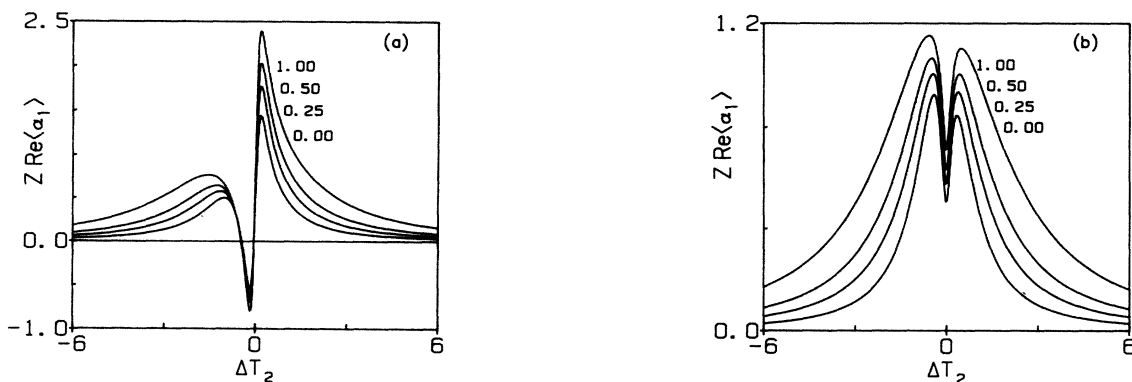


FIG. 15. $Z \text{Re}\langle\alpha_1\rangle_{ud}$ for the same parameters as in Figs. 9(a) and 9(b).

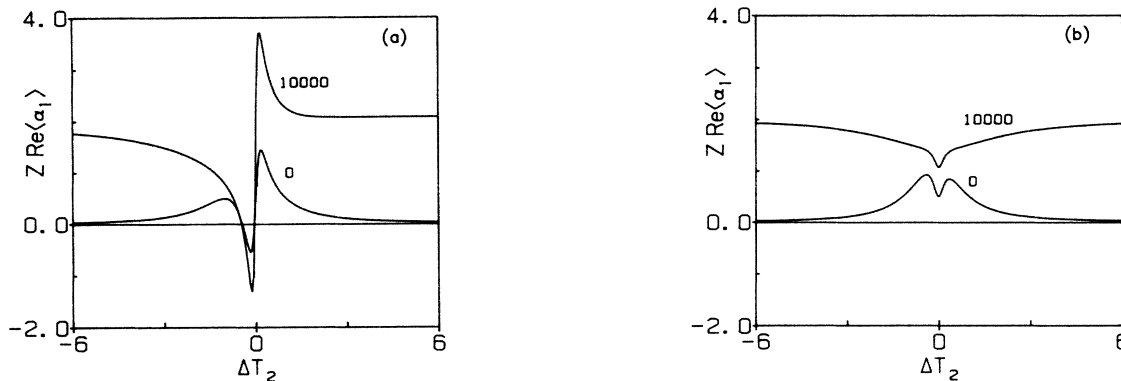


FIG. 16. Same as Fig. 15 except for the homogeneously ($wT_2=0$) and inhomogeneously ($wT_2=10000$) broadened limits.

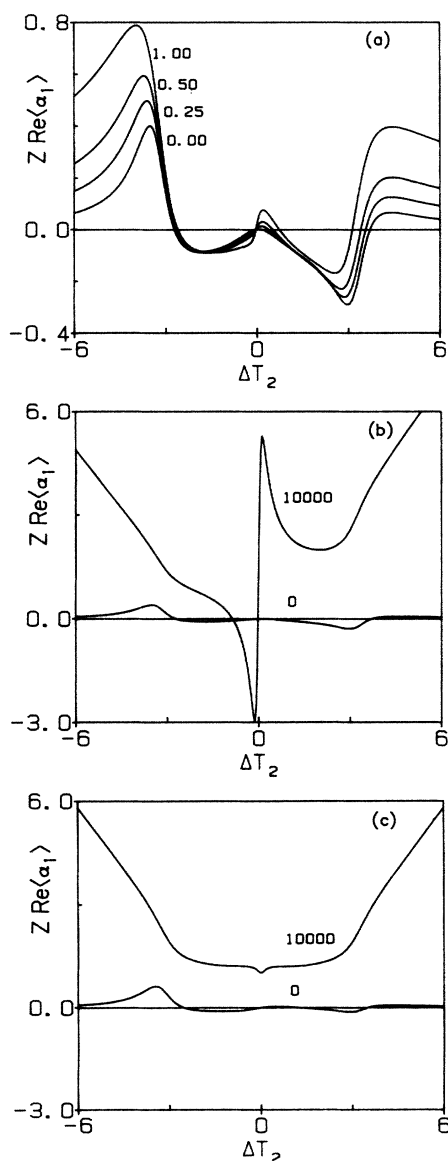


FIG. 17. (a) $Z\text{Re}\langle\alpha_1\rangle_{\text{ud}}$ for the same parameters as in Fig. 10(a). (b) and (c) the same as Figs. 10(a) and 10(b) except for the unidirectional case scaled by Z and for the homogeneously ($wT_2=0$) and inhomogeneously ($wT_2=10000$) broadened limits.

and 10(b) for small Doppler widths the results are similar, illustrated now in Fig. 17(a) only for the Stark-shifted case. However, in the Doppler limit, shown in Figs. 17(b) and 17(c), we again see the characteristic dispersive shape as in Fig. 16(a) and the broad shoulders with a much smaller dip than seen in Fig. 16(b).

VII. CONCLUSIONS

We have shown how the simple analytical model of a Lorentzian velocity distribution for the Doppler broadening can be included for copropagating and counter-propagating pump and probe beams and have looked at the transition from homogeneous to extreme Doppler broadening for the probe absorption with an arbitrarily intense field. The unidirectional and bidirectional cases are significantly different. We find that for the bidirectional case for weak intensities the spectrum is narrow for any amount of Doppler broadening but even a degree of broadening as small as $1/2T_2$ fills in coherent dips. For strong intensities the homogeneously broadened spectrum, characterized by a width of about twice the Rabi frequency, narrows in the Doppler limit to a non-power-broadened width of $2/T_2$. This limit is reached only when the Doppler broadening is significantly larger than the Rabi frequency. This is true in all level and coherence timescale regimes. In this limit Stark shifts acting similarly to detunings merely displace the Doppler-free Lorentzian from its nonzero value and all asymmetries vanish. In contrast, the unidirectional results are similar to those for one-photon inhomogeneous broadening. In this case the spectrum never becomes Doppler free and coherent dips are not filled in.

ACKNOWLEDGMENTS

It is a pleasure to thank David Holm for helpful discussions. This work has been supported in part by the United States Office of Naval Research under contract No. N00014-81-K-0754 and in part by the Air Force Office of Scientific Research and the Army Research Office under contract No. F49620-85-C-0039.

APPENDIX A: COUNTERPROPAGATING PUMP AND PROBE

In this appendix we derive the equations for the probe-absorption coefficient α_1 averaged over Doppler broadening,

$$\langle \alpha_1 \rangle = \int \alpha_1(v) W(v) dv \quad (\text{A1})$$

for the bidirectional case. All the averages are done assuming the Lorentzian velocity distribution $W(v)$ of Eq. (30). We need to express α_1 [Eq. (26)] as a function of velocity. As discussed in Sec. III for a counterpropagating pump and probe we replace v_1 by $v_1 - Kv$ and v_2 by $v_2 + Kv$ where we now let v represent the z component of velocity for typographical simplicity. Having made these substitutions we have (setting $x = 2Kv$)

$$\Delta(x)' = v_2 + Kv - (v_1 - Kv) = \Delta + x,$$

$$\Delta_2(x)' = \omega - 2(v_2 + Kv) + \omega_S I_2 = \Delta_2 - x,$$

$$\mathcal{D}_1(x)' = \mathcal{D}_1 = [\gamma + i(\Delta_2 - \Delta)]^{-1},$$

$$\mathcal{D}_2(x)' = [\gamma + i(\Delta_2 - x)]^{-1},$$

$$\mathcal{D}_3(x)' = [\gamma + i(\Delta_2 - \Delta - 2x)]^{-1},$$

$$\mathcal{L}_2(x)' = [1 + (\Delta_2 - x)^2 / \gamma^2]^{-1},$$

and

$$\mathcal{F}(x)' = [1 + iT_1(\Delta + x)]^{-1}, \quad (\text{A2})$$

where the primes indicate the substitutions for v_1 and v_2 have been made. Note that \mathcal{D}_1 remains independent of x , i.e., it is Doppler free. Using Eq. (30) we have for any function $g(v)$

$$\langle g \rangle_{\text{DB}} = \int_{-\infty}^{\infty} dv W(v) g(v)' = \frac{w}{\pi} \int_{-\infty}^{\infty} dx \frac{g(x)'}{w^2 + x^2}, \quad (\text{A3})$$

where $w = 2Ku$ is the width of the velocity distribution in frequency units. Substituting Eq. (26) into Eq. (A3) we obtain

$$\begin{aligned} \langle \alpha_1 \rangle_{\text{bd}} = & -\frac{iK_1 N}{4\epsilon_0} (k_{aa} + b_{bb}) + \alpha_0 (2I_2 \gamma \mathcal{D}_1 - i\omega_S T_1) \langle a_{11} \rangle - i\alpha_0 \omega_S I_2^2 \mathcal{D}_1 \langle a_{22} \rangle \\ & + \alpha_0 I_2^2 (i\omega_S T_1 - I_2 \gamma \mathcal{D}_1) \left[\gamma \mathcal{D}_1 \langle a_0 \rangle + \langle a_1 \rangle + \frac{i\omega_S I_2}{2\gamma} (\langle a_2 \rangle - \gamma \mathcal{D}_1 \langle a_3 \rangle) \right], \end{aligned} \quad (\text{A4})$$

where bd stands for bidirectional. The a_k representing the functions over which the integral is performed are

$$a_{11} = (1 + I_2^2 \mathcal{L}_2')^{-1}, \quad (\text{A5})$$

$$a_{22} = \gamma \mathcal{D}_2' a_{11}, \quad (\text{A6})$$

$$a_0 = a_{11} \mathcal{F}' / \left[1 + \frac{\gamma}{2} I_2^2 \mathcal{F}' (\mathcal{D}_1 + \mathcal{D}_3') \right], \quad (\text{A7})$$

$$a_1 = \gamma \mathcal{D}_2^* a_0, \quad (\text{A8})$$

$$a_2 = \gamma^2 \mathcal{D}_2^* \mathcal{D}_3^* a_0, \quad (\text{A9})$$

and

$$a_3 = \gamma \mathcal{D}_2' a_0. \quad (\text{A10})$$

We thus need only to evaluate the integral in Eq. (A3) for the expressions (A5) through (A10) to obtain the complete answer for $\langle \alpha_1 \rangle_{\text{bd}}$. The integrals are most easily evaluated in the complex plane using the residue theorem and thus for each one we need to evaluate the integrand at each of its poles. For the sake of typographical simplicity we drop the primes in the expressions which follow.

First we determine a_{11} as a function of x ,

$$a_{11}(x) = (1 + I_2^2 \mathcal{L}_2)^{-1} = \frac{\gamma^2 + (\Delta_2 - x)^2}{\gamma'^2 + (\Delta_2 - x)^2}, \quad (\text{A11})$$

where

$$\gamma' = \gamma(1 + I_2^2)^{1/2}. \quad (\text{A12})$$

Substituting this into Eq. (A3) and moving into the complex plane we obtain

$$\langle a_{11} \rangle = \frac{w}{\pi} \int_{-\infty}^{\infty} \frac{dz}{z^2 + w^2} \frac{(\Delta_2 - z)^2 + \gamma^2}{(\Delta_2 - z)^2 + \gamma'^2}. \quad (\text{A13})$$

The four poles of the integrand are located at $z = \pm i\omega$ and $z = \Delta_2 \pm i\gamma'$. We close the contour in the lower half plane and evaluate the residues at $z = -i\omega$ and $z = \Delta_2 - i\gamma'$. We then obtain

$$\langle a_{11} \rangle = \frac{M(i\omega, \gamma)}{M(i\omega, \gamma')} + \frac{w}{\gamma'} \frac{\gamma^2 - \gamma'^2}{M(-i\gamma', w)}, \quad (\text{A14})$$

where

$$M(z, x) = (\Delta_2 + z)^2 + x^2. \quad (\text{A15})$$

We proceed in the same manner to determine $\langle a_{22} \rangle$. First we obtain $a_{22}(x)$,

$$a_{22}(x) = \frac{\gamma[\gamma - i(\Delta_2 - x)]}{(x - \Delta_2 - i\gamma')(x - \Delta_2 + i\gamma')}. \quad (\text{A16})$$

Substituting into Eq. (A3) and evaluating at the poles $z = -i\omega$ and $z = \Delta_2 - i\gamma'$, we obtain

$$\langle a_{22} \rangle = -i\gamma \left[\frac{\Delta_2 + i(\gamma + w)}{M(i\omega, \gamma')} + \frac{iw}{\gamma'} \frac{\gamma + \gamma'}{M(-i\gamma', w)} \right]. \quad (\text{A17})$$

The final four averages require us to determine $a_0(x)$

which is more involved due to the complexity of a_0 . We can write a_0 as

$$a_0 = \frac{(\Delta_2 - x)^2 + \gamma^2}{(\Delta_2 - x)^2 + \gamma'^2} [1 + iT_1(\Delta + x)]^{-1} \chi, \quad (\text{A18})$$

where

$$\chi = \left[1 + \frac{\gamma}{2} I_2^2 \frac{\mathcal{D}_1 + \mathcal{D}_3^*}{1 + iT_1(\Delta + x)} \right]^{-1} \quad (\text{A19})$$

Then χ as a function of x becomes

$$\chi = \frac{[\gamma - i(\Delta_2 - \Delta - 2x)][1 + iT_1(\Delta + x)]}{[\gamma - i(\Delta_2 - \Delta - 2x)][1 + iT_1(\Delta + x)] + \gamma I_2^2 \mathcal{D}_1 [\gamma + i(\Delta + x)]}. \quad (\text{A20})$$

In order to determine the poles of a_0 we need to factor the denominator of χ . We do this using the quadratic formula to obtain

$$\text{den}(\chi) = -2T_1(x - \beta_-)(x - \beta_+), \quad (\text{A21})$$

where

$$\beta_{\pm} = \frac{i(2\mathcal{D}_{3h}^* + T_1\mathcal{F}_h + \gamma I_2^2 \mathcal{D}_1 \mathcal{D}_{3h}^* \mathcal{F}_h)}{4T_1 \mathcal{D}_{3h}^* \mathcal{F}_h} \pm \frac{1}{2} \left[\frac{2[1 + \gamma I_2^2 \mathcal{D}_1 \mathcal{D}_{3h}^* \mathcal{F}_h (\gamma + i\Delta)]}{T_1 \mathcal{D}_{3h}^* \mathcal{F}_h} - \left(\frac{2\mathcal{D}_{3h}^* + T_1\mathcal{F}_h + \gamma I_2^2 \mathcal{D}_1 \mathcal{D}_{3h}^* \mathcal{F}_h}{2T_1 \mathcal{D}_{3h}^* \mathcal{F}_h} \right)^2 \right]^{1/2}, \quad (\text{A22})$$

and

$$\mathcal{D}_{3h}^* = [\gamma - i(\Delta_2 - \Delta)]^{-1} \quad (\text{A23})$$

and

$$\mathcal{F}_h = (1 + iT_1\Delta)^{-1}, \quad (\text{A24})$$

which are the standard homogeneous expressions for \mathcal{D}_3^* and \mathcal{F} . Using the factorization in Eq. (A21) we can then express χ as

$$\chi = -\frac{1}{2T_1 \mathcal{D}_{3h}^* \mathcal{F}_h} \left[\frac{(1 + 2i\mathcal{D}_{3h}^* x)(1 + iT_1\mathcal{F}_h x)}{(x - \beta_-)(x - \beta_+)} \right]. \quad (\text{A25})$$

Finally, we obtain

$$a_0(x) = -\frac{1}{2T_1 \mathcal{D}_{3h}^*} \frac{[(\Delta_2 - x)^2 + \gamma^2](1 + 2i\mathcal{D}_{3h}^* x)}{[(\Delta_2 - x)^2 + \gamma'^2](x - \beta_-)(x - \beta_+)}. \quad (\text{A26})$$

Substituting this into the integral of Eq. (A3) we then obtain

$$\langle a_0 \rangle = -\frac{wB}{\pi} \int_{-\infty}^{\infty} dz \frac{[(\Delta_2 - z)^2 + \gamma^2](1 + 2i\mathcal{D}_{3h}^* z)}{(z^2 + w^2)[(\Delta_2 - z)^2 + \gamma'^2](z - \beta_-)(z - \beta_+)}, \quad (\text{A27})$$

where

$$B = \frac{1}{2T_1 \mathcal{D}_{3h}^*}. \quad (\text{A28})$$

The location of the poles at β_{\pm} is not immediately obvious, however, graphical analysis shows them to always be in the upper half plane for any parameters of interest. Thus, by closing the contour in the lower plane we are left with only the two poles at $z = -iw$ and $z = \Delta_2 - i\gamma'$. This finally gives us

$$\langle a_0 \rangle = -B \left[\frac{M(iw, \gamma)G(-iw)}{M(iw, \gamma')} + \frac{w}{\gamma'} \frac{(\gamma^2 - \gamma'^2)G(\Delta_2 - i\gamma')}{M(-i\gamma', w)} \right], \quad (\text{A29})$$

where

$$G(z) = \frac{1 + 2i\mathcal{D}_{3h}^* z}{(z - \beta_-)(z - \beta_+)}. \quad (\text{A30})$$

Having evaluated a_0 we can now easily evaluate the remaining three terms. To obtain a_1 we note that it is merely

$\gamma \mathcal{D}_2^* a_0$ so we can write it as

$$a_1(x) = -i\gamma B \frac{(\Delta_2 - x - i\gamma)(1 + 2i\mathcal{D}_{3h}^*)}{[(\Delta_2 - x)^2 + \gamma'^2](x - \beta_-)(x - \beta_+)} . \quad (\text{A31})$$

Following the same procedure as before we substitute this into Eq. (A3) and after closing the contour in the lower half plane and enclosing the two poles at $z = -iw$ and $z = \Delta_2 - i\gamma'$ we obtain

$$\langle a_1 \rangle = -i\gamma B \left[\frac{\Delta_2 + i(w - \gamma)}{M(iw, \gamma')} G(-iw) + \frac{iw}{\gamma'} (\gamma' - \gamma) \frac{G(\Delta_2 - i\gamma')}{M(-i\gamma', w)} \right] . \quad (\text{A32})$$

Using the same procedure for a_2 we can write

$$a_2(x) = -\gamma^2 B \frac{(\Delta_2 - x - i\gamma)(1 + 2i\mathcal{D}_{3h}^* x)}{(2x - \Delta_2 + \Delta - i\gamma)[(x - \Delta_2)^2 + \gamma'^2](x - \beta_-)(x - \beta_+)} \quad (\text{A33})$$

and

$$\langle a_2 \rangle = \gamma^2 B \left[\frac{[\Delta_2 + i(w - \gamma)]G(-iw)}{[\Delta_2 - \Delta + i(2w + \gamma)]M(iw, \gamma')} - \frac{iw}{\gamma'} \frac{(\gamma' - \gamma)G(\Delta_2 - i\gamma')}{[\Delta_2 + \Delta - i(2\gamma' + \gamma)]M(-i\gamma', w)} \right] . \quad (\text{A34})$$

Repeating the procedure a final time for a_3 we obtain

$$a_3(x) = i\gamma B \frac{(\Delta_2 - x + i\gamma)(1 + 2i\mathcal{D}_{3h}^* x)}{[(\Delta_2 - x)^2 + \gamma'^2](x - \beta_-)(x - \beta_+)} \quad (\text{A35})$$

and

$$\langle a_3 \rangle = i\gamma B \left[\frac{\Delta_2 + i(w + \gamma)}{M(iw, \gamma')} G(-iw) + \frac{iw}{\gamma'} (\gamma' + \gamma) \frac{G(\Delta_2 - i\gamma')}{M(-i\gamma', w)} \right] . \quad (\text{A36})$$

Using the expressions for the $\langle a_n \rangle$ in Eq. (A4) we obtain Eq. (38).

$$\langle \alpha_1 \rangle_{\text{ud}} = -\frac{iK_1 N}{4\epsilon_0} (k_{aa} + k_{bb}) + \alpha_0 (-i\omega_S T_1 \langle b_{11} \rangle + 2I_2 \langle b_{22} \rangle - iI_2^2 \langle b_{33} \rangle) - I_2^2 \mathcal{F}(\Delta) \alpha_0 \left[I_2 \langle b_1 \rangle - i\omega_S T_1 \langle b_2 \rangle + \frac{iI_2^2}{2} (\langle b_3 \rangle - \langle b_4 \rangle) + \frac{\omega_S T_1 I_2}{2} (\langle b_5 \rangle - \langle b_6 \rangle) \right] , \quad (\text{B2})$$

where ud stands for unidirectional and the b_k are given by

$$b_{11} = (1 + I_2^2 \mathcal{L}_2')^{-1} , \quad (\text{B3})$$

$$b_{22} = \gamma \mathcal{D}_1' b_{11} , \quad (\text{B4})$$

$$b_{33} = \gamma \omega_S \mathcal{D}_1' \mathcal{D}_2' b_{11} , \quad (\text{B5})$$

$$b_1 = \frac{\gamma^2 \mathcal{D}_1' (\mathcal{D}_1' + \mathcal{D}_3^{*'}) b_{11}}{1 + \frac{\gamma}{2} I_2^2 \mathcal{F}(\mathcal{D}_1' + \mathcal{D}_3^{*'})} , \quad (\text{B6})$$

APPENDIX B: COPROGAGATING PUMP AND PROBE

Now we proceed in the same manner to derive Eq. (45) for the coprogagating pump and probe. For this configuration we replace v_1 by $v_1 + Kv$ and v_2 by $v_2 + Kv$. Making these substitutions and again setting $x = 2Kv$ we have

$$\Delta(x)' = v_2 + Kv - (v_1 + Kv) = \Delta ,$$

$$\Delta_2(x)' = \Delta_2 - x ,$$

$$\mathcal{D}_1(x)' = [\gamma + i(\Delta_2 + \Delta - x)]^{-1} ,$$

$$\mathcal{D}_2(x)' = [\gamma + i(\Delta_2 - x)]^{-1} ,$$

$$\mathcal{D}_3(x)' = [\gamma + i(\Delta_2 - \Delta - x)]^{-1} ,$$

$$\mathcal{L}_2(x)' = [1 + (\Delta_2 - x)^2 / \gamma'^2]^{-1} ,$$

and

$$\mathcal{F}(x)' = (1 + i\Delta T_1)^{-1} , \quad (\text{B1})$$

where once again the primes indicate the substitutions for v_1 and v_2 have been made. We note that for this case \mathcal{D}_1 is no longer Doppler free but Δ and therefore \mathcal{F} are. The expressions for Δ_2 , \mathcal{D}_2 , and \mathcal{L}_2 are the same as in the bi-directional case. Since \mathcal{D}_1 is no longer Doppler free, when we substitute Eq. (26) into Eq. (A3) we now obtain

$$b_2 = b_1 / \gamma \mathcal{D}_1' , \quad (\text{B7})$$

$$b_3 = \gamma^2 \omega_S \frac{\mathcal{D}_1' \mathcal{D}_2^{*'} \mathcal{D}_3^{*'} b_{11}}{1 + \frac{\gamma}{2} I_2^2 \mathcal{F}(\mathcal{D}_1' + \mathcal{D}_3^{*'})} , \quad (\text{B8})$$

$$b_4 = b_3 \mathcal{D}_1' / \mathcal{D}_3^{*'} , \quad (\text{B9})$$

$$b_5 = b_3 / \gamma \mathcal{D}_1' , \quad (\text{B10})$$

and

$$b_6 = b_4 / \gamma \mathcal{D}'_1. \quad (\text{B11})$$

We note that b_{11} is the same as a_{11} but we reevaluate it since for this case we close all the contours in the upper half plane. Proceeding as before, we determine each b_k as a function of x , substitute it into Eq. (A3), move into the complex plane, and determine the poles. Since the expressions for b_{11} , b_{22} , and b_{33} have the same two poles, we shall handle them as one group. Thus expressing them all as functions of x and dropping the primes we have

$$b_{11}(x) = \frac{(x - \Delta_2)^2 + \gamma^2}{(x - \Delta_2)^2 + \gamma'^2}, \quad (\text{B12})$$

$$b_{22}(x) = \frac{i\gamma}{x - \Delta_2 - \Delta + i\gamma} \frac{(x - \Delta_2)^2 + \gamma^2}{(x - \Delta_2)^2 + \gamma'^2}, \quad (\text{B13})$$

and

$$b_{33}(x) = \frac{-\gamma\omega_S(x - \Delta_2 - i\gamma)}{(x - \Delta_2 - \Delta + i\gamma)[(x - \Delta_2)^2 + \gamma'^2]}. \quad (\text{B14})$$

When these three expressions are each substituted into Eq. (A3) they each have two poles in the upper half plane. These are for $z = iw$ and $z = \Delta_2 + i\gamma'$. Evaluating each of the residues at these poles and taking the sum we obtain the following expressions for the averages:

$$\langle b_{11} \rangle = \frac{M(-iw, \gamma)}{M(-iw, \gamma')} + \frac{w}{\gamma'} \frac{\gamma^2 - \gamma'^2}{M(i\gamma', w)}, \quad (\text{B15})$$

$$\langle b_{22} \rangle = \frac{i\gamma}{[-\Delta_2 - \Delta + i(w + \gamma)]} \frac{M(-iw, \gamma)}{M(-iw, \gamma')} + \frac{w}{\gamma'} \frac{i\gamma(\gamma^2 - \gamma'^2)}{[-\Delta + i(\gamma' + \gamma)]M(i\gamma', w)}, \quad (\text{B16})$$

and

$$\langle b_{33} \rangle = \frac{-\omega_S\gamma[-\Delta_2 + i(w - \gamma)]}{[-\Delta_2 - \Delta + i(w + \gamma)]M(-iw, \gamma')} + \frac{w}{\gamma'} \frac{-i\omega_S\gamma(\gamma' - \gamma)}{[-\Delta_2 - \Delta + i(\gamma' + \gamma)]M(i\gamma', w)}. \quad (\text{B17})$$

As in the previous case we need to factor the complex denominator in Eq. (B8) in order to evaluate the remaining integrals. We again let $\chi = \frac{1}{2}[2 + \gamma I_2^2 \mathcal{F}(\mathcal{D}_1 + \mathcal{D}_3^*)]^{-1}$ which when expressed as a function of x becomes

$$\chi_{\text{ud}} = \frac{(x - \Delta_2)^2 - (\Delta - i\gamma)^2}{(x - \Delta_2)^2 - (\Delta - i\gamma)^2 + iI_2^2\gamma\mathcal{F}(\Delta - i\gamma)}. \quad (\text{B18})$$

We then factor the denominator to obtain

$$\chi_{\text{ud}} = \frac{(x - \Delta_2)^2 - (\Delta - i\gamma)^2}{(x - \beta_1)(x - \beta_2)}, \quad (\text{B19})$$

where now

$$\beta_{1,2} = \Delta_2 \pm [(\Delta - i\gamma)(\Delta - i\gamma - iI_2^2\gamma\mathcal{F})]^{1/2}. \quad (\text{B20})$$

All of the remaining integrals thus have poles at β_1 and β_2 . These poles are not always in one half plane as is the case for the bidirectional configuration. Instead their locations are dependent on Δ , T_1 , γ , and I_2 . When

$$\Delta(\Delta + \Delta_p)(\Delta - \Delta_p) < 0, \quad (\text{B21})$$

where

$$\Delta_p = \frac{[I_2^2(\gamma T_1 - 1)/2 - 1]^{1/2}}{T_1}, \quad (\text{B22})$$

the β_1 pole is in the upper half plane while the β_2 pole is in the lower half plane and otherwise the poles switch planes. In the expressions which follow we close all the contours in the upper plane, assume that Eq. (B21) is true and that the β_1 pole is in the upper half plane. When Eq. (B21) does not hold we merely replace β_1 with β_2 and vice versa.

Using Eq. (B19) for χ we express $b_1 - b_6$ as functions of x ,

$$b_1(x) = i\gamma^2(2\gamma + i\Delta) \frac{(x - \Delta_2 + \Delta - i\gamma)(x - \Delta_2 + i\gamma)}{(x - \Delta_2 - \Delta + i\gamma)(x - \beta_1)(x - \beta_2)[(x - \Delta_2)^2 + \gamma'^2]}, \quad (\text{B23})$$

$$b_2(x) = \gamma(2\gamma + i\Delta) \frac{(x - \Delta_2 + \Delta - i\gamma)(x - \Delta_2 + i\gamma)}{(x - \beta_1)(x - \beta_2)[(x - \Delta_2)^2 + \gamma'^2]}, \quad (\text{B24})$$

$$b_3(x) = -i\gamma^2\omega_S \frac{x - \Delta_2 + i\gamma}{(x - \beta_1)(x - \beta_2)[(x - \Delta_2)^2 + \gamma'^2]}, \quad (\text{B25})$$

$$b_4(x) = -i\gamma^2\omega_S \frac{(x - \Delta_2 + \Delta - i\gamma)(x - \Delta_2 - i\gamma)}{(x - \Delta_2 - \Delta + i\gamma)(x - \beta_1)(x - \beta_2)[(x - \Delta_2)^2 + \gamma'^2]}, \quad (\text{B26})$$

$$b_5(x) = -\gamma\omega_S \frac{(x - \Delta_2 - \Delta + i\gamma)(x - \Delta_2 + i\gamma)}{(x - \beta_1)(x - \beta_2)[(x - \Delta_2)^2 + \gamma'^2]}, \quad (\text{B27})$$

and

$$b_6(x) = -\gamma\omega_S \frac{(x - \Delta_2 + \Delta - i\gamma)(x - \Delta_2 - i\gamma)}{(x - \beta_1)(x - \beta_2)[(x - \Delta_2)^2 + \gamma'^2]}. \quad (\text{B28})$$

Substituting Eqs. (B23)–(B28) each into Eq. (A3) and going into the complex plane, we see that while Eq. (B21) holds they all have the same three poles in the upper half plane at $z = \beta_1$, $z = iw$ and $z = \Delta_2 + i\gamma'$. Evaluating the residues at these poles and summing the results we obtain the following averages:

$$\langle b_1 \rangle = \frac{i\gamma^2(2\gamma + i\Delta)[-\Delta_2 + \Delta + i(w - \gamma)][-\Delta_2 + i(w + \gamma)]}{[-\Delta_2 - \Delta + i(w + \gamma)]M(-iw, \gamma')N(iw)} - \frac{w}{\gamma'} \frac{\gamma^2(2\gamma + i\Delta)(\gamma' + \gamma)[\Delta + i(\gamma' - \gamma)]}{[-\Delta + i(\gamma' + \gamma)]M(i\gamma', w)N(\Delta_2 + i\gamma')}$$

$$- 2w \frac{\gamma^2(2\gamma + i\Delta)(-\Delta_2 + \Delta - i\gamma + \beta_1)(-\Delta_2 + i\gamma + \beta_1)}{(-\Delta_2 - \Delta + i\gamma + \beta_1)M(-\beta_1, \gamma')Q}, \quad (\text{B29})$$

$$\langle b_2 \rangle = \frac{\gamma(2\gamma + i\Delta)[-\Delta_2 + \Delta + i(w - \gamma)][-\Delta_2 + i(w + \gamma)]}{M(-iw, \gamma')N(iw)} + \frac{iw}{\gamma'} \frac{\gamma(2\gamma + i\Delta)(\gamma' + \gamma)[\Delta + i(\gamma' - \gamma)]}{M(i\gamma', w)N(\Delta_2 + i\gamma')}$$

$$+ 2iw \frac{\gamma(2\gamma + i\Delta)(-\Delta_2 + \Delta - i\gamma + \beta_1)(-\Delta_2 + i\gamma + \beta_1)}{M(-\beta_1, \gamma')Q}, \quad (\text{B30})$$

$$\langle b_3 \rangle = -i \frac{\gamma^2\omega_S[-\Delta_2 + i(w + \gamma)]}{M(-iw, \gamma')N(iw)} + \frac{w}{\gamma'} \frac{\gamma^2\omega_S(\gamma' + \gamma)}{M(i\gamma', w)N(\Delta_2 + i\gamma')} + 2w \frac{\gamma^2\omega_S(-\Delta_2 + i\gamma + \beta_1)}{M(-\beta_1, \gamma')Q}, \quad (\text{B31})$$

$$\langle b_4 \rangle = \frac{-i\gamma^2\omega_S[-\Delta_2 + \Delta + i(w - \gamma)][-\Delta_2 + i(w - \gamma)]}{[-\Delta_2 - \Delta + i(w + \gamma)]M(-iw, \gamma')N(iw)} + \frac{w}{\gamma'} \frac{\gamma^2\omega_S(\gamma' - \gamma)[\Delta + i(\gamma' - \gamma)]}{[-\Delta + i(\gamma' + \gamma)]M(i\gamma', w)N(\Delta_2 + i\gamma')}$$

$$+ 2w \frac{\gamma^2\omega_S(-\Delta_2 + \Delta - i\gamma + \beta_1)(-\Delta_2 - i\gamma + \beta_1)}{(-\Delta_2 - \Delta + i\gamma + \beta_1)M(-\beta_1, \gamma')Q}, \quad (\text{B32})$$

$$\langle b_5 \rangle = - \frac{\gamma\omega_S[-\Delta_2 - \Delta + i(w + \gamma)][-\Delta_2 + i(w + \gamma)]}{M(-iw, \gamma')N(iw)} - \frac{iw}{\gamma'} \frac{\gamma\omega_S(\gamma' + \gamma)[-\Delta + i(\gamma' + \gamma)]}{M(i\gamma', w)N(\Delta_2 + i\gamma')}$$

$$- 2iw \frac{\gamma\omega_S(-\Delta_2 - \Delta + i\gamma + \beta_1)(-\Delta_2 + i\gamma + \beta_1)}{M(-\beta_1, \gamma')Q}, \quad (\text{B33})$$

and

$$\langle b_6 \rangle = - \frac{\gamma\omega_S[-\Delta_2 + \Delta + i(w - \gamma)][-\Delta_2 + i(w - \gamma)]}{M(-iw, \gamma')N(iw)}$$

$$- \frac{iw}{\gamma'} \frac{\gamma\omega_S(\gamma' - \gamma)[\Delta + i(\gamma' - \gamma)]}{M(i\gamma', w)N(\Delta_2 + i\gamma')}$$

$$- 2iw \frac{\gamma\omega_S(-\Delta_2 + \Delta + i\gamma + \beta_1)(-\Delta_2 - i\gamma + \beta_1)}{M(-\beta_1, \gamma')Q} \quad (\text{B34})$$

In Eqs. (B29)–(B34), $M(z, x)$ is given in Eq. (A15),

$$N(z) = (z - \beta_1)(z - \beta_2) \quad (\text{B35})$$

and

$$Q = (\beta_1 - \beta_2)(\beta_1^2 + w^2). \quad (\text{B36})$$

Equations (B29)–(B34) hold while Eq. (B21) is true. The equivalent expressions when it is not true are the same except that β_1 and β_2 are interchanged. Using these equations for the $\langle b_k \rangle$ in Eq. (B2) we obtain the results of Eq. (45).

¹N. Bloembergen and M. D. Levenson, in *High Resolution Spectroscopy*, Vol. 13 of *Topics in Applied Physics*, edited by K. Shimoda (Springer-Verlag, Berlin, 1976).

²G. Grynberg, B. Cagnac, and F. Biraben, in *Coherent Non-linear Optics*, Vol. 21 of *Topics in Current Physics*, edited by M. S. Feld and V. S. Letokhov (Springer-Verlag, Berlin, 1980).

³W. K. Bischel, P. J. Kelley, and C. K. Rhodes, *Phys. Rev. Lett.* **34**, 300 (1975); *Phys. Rev. A* **13**, 1817 (1976).

⁴B. A. Capron, A. S. Marathay, and M. Sargent III, *Opt. Lett.* **11**, 70 (1986).

⁵M. Sargent III, S. Ovadia, and M. S. Lu, *Phys. Rev. A* **32**, 1596 (1985).

⁶B. R. Mollow, *Phys. Rev. A* **5**, 2217 (1972).

⁷E. V. Baklanov and V. P. Chebotayev, *Zh. Eksp. Teor. Fiz.* **60**, 552 (1971) [*Sov. Phys.—JETP* **33**, 300 (1971)].

⁸E. V. Baklanov and V. P. Chebotayev, *Zh. Eksp. Teor. Fiz.* **61**, 922 (1971) [*Sov. Phys.—JETP* **34**, 490 (1972)].

⁹M. Sargent III, *Phys. Rep.* **43C**, 223 (1978).

¹⁰D. A. Holm, M. Sargent III, and L. M. Hoffer, *Phys. Rev. A* **32**, 963 (1985).

¹¹D. A. Holm and M. Sargent III, in *Coherence and Quantum Optics V*, edited by L. Mandel and E. Wolf (Plenum, New York, 1984).

¹²M. Takatsuji, *Phys. Rev. A* **4**, 808 (1971).

¹³B. R. Mollow, *Phys. Rev. A* **4**, 1666 (1971).

¹⁴M. Sargent III, M. O. Scully, and W. E. Lamb, *Laser Physics* (Addison-Wesley, Reading, Mass., 1974), Chap. 10.

¹⁵A nonperturbative power-broadened absorption coefficient for the case of two waves of equal intensity appears in G. Grynberg, M. Devaux, C. Flytzanis, and B. Cagnac, *J. Phys.* **41**, 931 (1980).